Failure Analysis of Laminated Composite Plates with Two Parallel Pin-loaded Holes

AKIN ATAŞ* AND NURETTIN ARSLAN
Department of Mechanical Engineering, Balikesir University
Balikesir, Turkey

FARUK SEN
Department of Mechanical Engineering, Aksaray University
Aksaray, Turkey

ABSTRACT: The aim of this study is to research the failure loads and failure modes of laminated woven-glass–polyester composite plates with two parallel circular holes, which are subjected to traction forces by two rigid pins. The failure behavior of two parallel pin-loaded composite plates has been observed both experimentally and numerically with different geometries and fiber orientations. While the plate width to hole diameter ratio (W/D) was held constant; the distance from the free edge of the plate to hole diameter ratio (E/D) was changed from 1 to 5, and the distance between two parallel holes to hole diameter ratio (M/D) was varied from 2 to 5. Two different ply orientations were also investigated as $[0^\circ]_8$ and $[0^\circ_2/60^\circ_2/]_s$. In a numerical study, a three-dimensional finite element method (FEM) was used with the assistance of a LUSAS 13.6 finite element analysis program. Good agreement has been shown between experimental and numerical results.

KEY WORDS: composite plate, bearing strength, parallel pin loading, failure analysis.

INTRODUCTION

COMPOSITES HAVE EMERGED as important materials because of their light weight, high specific stiffness, high specific strength, excellent fatigue resistance, and outstanding corrosion resistance compared to most common metallic alloys, such as steel and aluminum alloys [1]. Owing to these advantages, composite materials are widely used especially in aircraft, the automotive industry, and aerospace and civil engineering applications. These applications usually necessitate the joining of composites either to other composites or to other materials. For assembling these materials, mechanical fastening is a common technology and pin or bolt joints are indispensable in these structural components because of their low cost, simplicity, and facilitation of disassembly for repair. Therefore, particular attention should be shown to determine the failure strength and failure modes of these pinned or bolted connections [2,3].

On account of the importance of the problem, various research articles [3–6] on bearing strengths have been published, demonstrating that the failure mode is dependent on the

*Author to whom correspondence should be addressed. E-mail: akin@balikesir.edu.tr
Figures 1 and 5–8 appear in color online: http://jrp.sagepub.com

0731-6844/09/10 1265–12 $10.00/0 DOI: 10.1177/0731684408089493
© SAGE Publications 2009
Los Angeles, London, New Delhi and Singapore

width-to-diameter (W/D) and edge distance-to-diameter (E/D) ratios. Many investigators [4–11] have analyzed the dependence of bearing strength on specimen geometry, fiber orientation and materials that were used. Investigations have shown pin-loaded specimen failures on three basic modes: net-tension, shear-out, and bearing. Net-tension and shear-out failure modes occur when too low (W/D) and (E/D) ratio are used, respectively. These failure modes are catastrophic and can turn into the bearing mode by increasing the (E/D) and (W/D) ratios [3,7].

Camanho and Lambert [12] developed a new methodology to predict the final failure and failure mode of mechanically fastened joints in composite laminates. The elastic limit of the joint was predicted using ply strength and stress distribution in failure criteria. Final failure and failure mode were predicted using point or average stress models. The authors compared the predictions with experimental data and the results indicate that the methodology proposed can accurately predict failure loads. Whitworth et al. [13] performed an analysis to evaluate the bearing strength of pin-loaded composites using the Yamada–Sun failure criterion. Investigators observed a good correlation when evaluated as a function of edge distance to hole diameter and as a function of plate width to hole diameter. Okutan [14] conducted a numerical and experimental study to determine the failure of mechanically fastened fiber-reinforced laminated composite joints. Tests were carried out on single pinned joints in $[0/90/0]_s$ and $[90/0/90]_s$ laminated composites. Various geometric parameters were performed to obtain the failure characteristics of the pin-loaded composites. Damage accumulations in the laminates were evaluated by using Hashin's failure criteria and based on the results, ply orientation and geometries of composites could be crucial for pinned laminated composite joints. Karakuzu et al. [15] have investigated the effects of geometrical parameters, such as the edge distance-to-hole diameter ratio (E/D), plate width-to-hole diameter ratio (W/D), and the distance between two holes-to-diameter ratio (M/D), on the failure loads and failure modes in woven-glass–vinylester composite plates with two serial pin-loaded holes both experimentally and numerically. The numerical and experimental results showed that the ultimate load capacity of composite plates increased by increasing ratios (E/D), (W/D), and (M/D). Meanwhile, a method was presented for predicting the failure strength and failure mode of mechanically fastened fiber reinforced composite laminates by Chang et al. [16]. A computer code was developed which can be used to calculate the maximum load and the mode of failure of joints involving laminates with different ply orientations, different material properties, and different geometries. Parametric studies were also performed to evaluate the effects of joint geometry and ply orientation on the failure strength and on the failure mode. Furthermore, a failure analysis was performed to determine bearing strengths of mechanically fastened joints with single bolt in glass–epoxy laminated composite plates by Sayman et al. [17]. The experimental results showed that the magnitudes of bearing strengths in bolted joints were strictly influenced from increasing value of applied preload moments, changing of W/D and E/D ratios, and also ply orientations of laminated composite plates.

In the present study, the effects of geometrical parameters such as the edge distance-to-hole diameter ratio ($E/D = 1$–5), plate width-to-hole diameter ratio ($W/D = 8$), and the distance between two parallel holes-to-diameter ratio ($M/D = 2$–5) on the failure loads and failure modes in $[0^\circ]_8$ and $[0^\circ_2/60^\circ_2/]_s$ orientated woven-glass–polyester composite plates with two parallel pin-loaded holes were investigated. Analyses were performed both experimentally and numerically. During the numerical study, a commercial finite element package program LUSAS was used for considering Hashin failure criterion.

PROBLEM STATEMENT

The woven-glass–polyester composite specimen was designed with a length $L + E$, width W, and thickness t with two parallel circular holes of diameter D as shown in Figure 1. As seen in this figure, the holes are at a distance E from the free edge of the specimen. The L and D were fixed as 90 and 5 mm, respectively. Two pins were positioned at the center of the holes and a uniform tensile load P was applied to the specimen. The tensile load was also parallel to the specimen and it was symmetric with respect to the centerline.

The effects of the different geometries and fiber orientations on failure behavior were determined both experimentally and numerically. Studies were performed based on two different main parameters to observe failure response of two parallel pin-loaded composites. The first parameters were geometric, so edge distance-to-hole diameter ratio ($E/D = 1$–5), distance between two holes-to-diameter ratio ($M/D = 2$–5), and plate width-to-hole diameter ratio ($W/D = 8$) were considered. The other important parameter was fiber orientation. For this intention, laminated plates were arranged in two different stacking sequences $[0^\circ]_8$ and $[0^\circ_2/60^\circ_2/]_s$ and were named as Groups 1 and 2, respectively. These fiber orientations were also explained in Table 1. Each laminated plate was manufactured to connect eight laminas together symmetrically under pressure and heat. After the production process, the laminated plate had a nominal thickness of 1.9 mm at a volume fraction of 76%.

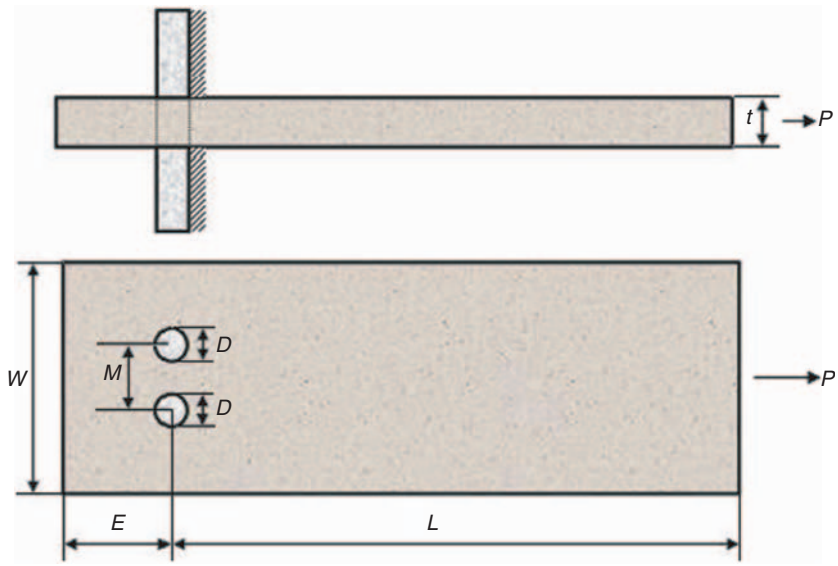

Figure 1. *Geometry of a composite specimen with two circular parallel holes.*

Table 1. Fiber orientation of laminated composites.

Group no.	Fiber orientation	Average thickness (mm)	Total number of laminas
1	$[0^\circ]_8$	1.9	8
2	$[0^\circ_2/60^\circ_2/]_s$	1.9	8

The experiments were carried out in tension mode on an Instron-1114 Tensile Test Machine at a crosshead speed of 1 mm/min. The experimental set-up for two parallel pinned-joints is illustrated schematically in Figure 2. As seen in this figure, the lower edge of the specimen was clamped and loaded from the steel pin by stretching the specimens. The apparatus was designed for different M/D ratios. The load versus pinned displacement curves for all composite configurations were drawn via a computer which was connected to a test machine. When pin-loaded composites have been overloaded under tensile loading, they fail on three basic modes, namely by net-tension, shear-out, and bearing modes, as shown in Figure 3. However, combinations of these failure modes are possible in practical applications [2,3,12]. The bearing strength of double pin-loaded composite specimens can be calculated as:

$$\sigma_b = \frac{P_{\max}}{2Dt} \tag{1}$$

where $P_{\max}$, D, and t are explained as tensile applied load, pin hole diameter, and thickness of the specimen, respectively.

PRODUCTION OF COMPOSITE PLATES

The woven-glass–polyester laminates used for the duration of the experimental studies were manufactured at Izoreel Firm in Izmir. Subsequent woven plies were placed one upon

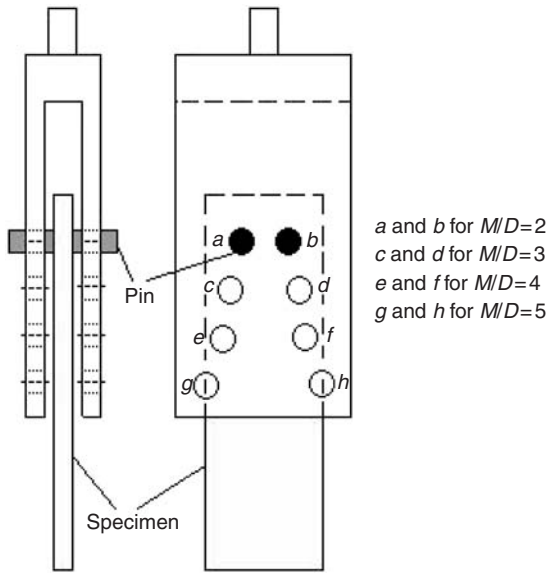

Figure 2. *Two parallel pinned-joint test fixture (for M/D = 2).*

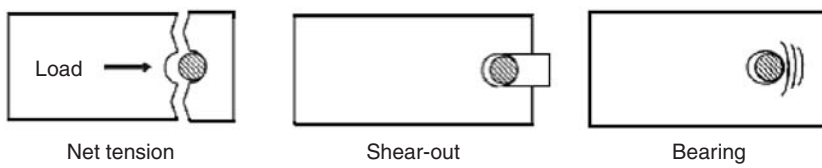

Figure 3. *Three basic failure modes of pin-loaded specimens.*

another to obtain stacking sequences ($[0^\circ]_8$ and $[0^\circ_2/60^\circ_2/]_s$). The mold and lay-up were covered with a release film to prevent the lay-up from bonding to the mold surface. After that resin-impregnated glass fibers were placed in the mold for curing. The glass-fiber and polyester were cured at 110°C under a pressure of 0.2 MPa. This temperature was held constant for 25 min. Finally, the laminates were cooled to room temperature. After the production process, the laminated composite plates had 1.90 mm average thickness with a fiber volume fraction of 76%.

MATERIAL CHARACTERIZATION

Mechanical tests were performed to determine the composite material properties. Three tests were carried out for each test type and average mechanical properties were calculated. Firstly, a tensile test were performed on the $[0]_8$ rectangular specimen to determine Young's modulus (E_1); Poisson's ratio (ν_{12}) and longitudinal tensile strength (X_t), according to ASTM D3039-76 [18]. Then, in-plane shear strength S of material was measured by using the Iosipescu shear test method. The loading fixture and geometry of Iosipescu testing specimen are illustrated in Figure 4 [3,14,19,20]. The dimensions of the specimen were chosen as $a = 80$ mm, $b = 20$ mm, $c = 10$ mm and $t_i = 1.9$ mm. A compression test was applied to the test fixture. After the failure test, S was calculated from:

$$S = \frac{F_{\max}}{t_i c} \tag{2}$$

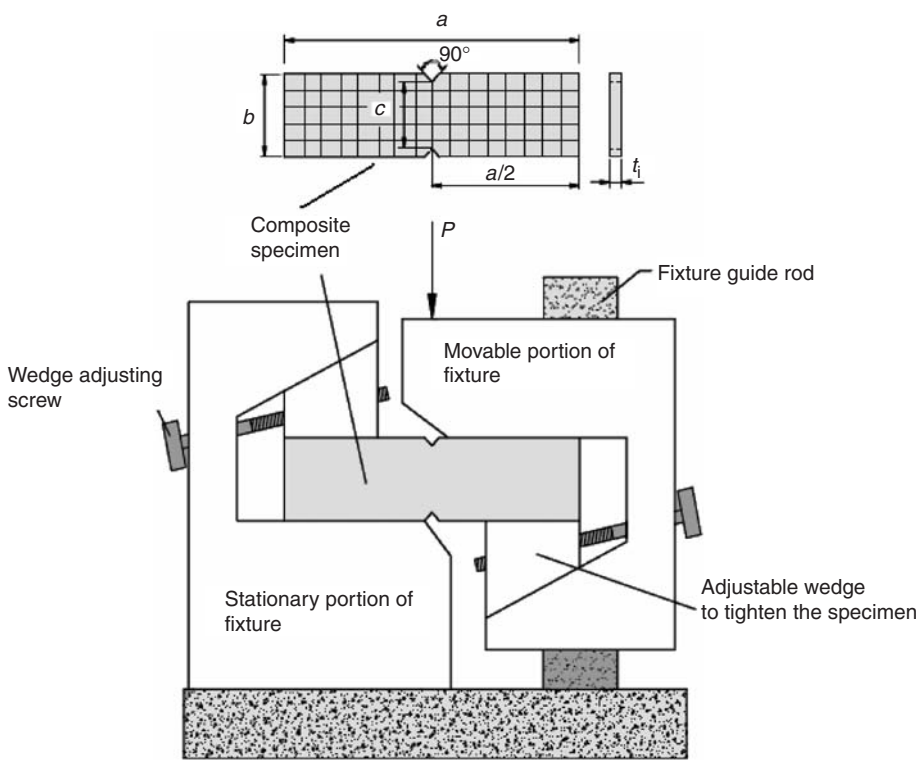

Figure 4. *Loading fixture and geometry of the Iosipescu testing specimen.*

Table 2. Mechanical properties of the woven-glass–polyester composite material.

$E_1 = E_2$ (GPa)	G_{12} (GPa)	ν_{12}	$X_t = Y_t$ (MPa)	$X_c = Y_c$ (MPa)	S (MPa)	V_f (%)
31.610	3.220	0.206	344.340	359.210	82.610	76

where $F_{\max}$ is the applied failure load to the Iosipescu test fixture. To obtain the shear modulus G_{12}, a specimen whose principal axis is at 45° with loading direction was considered and a strain gauge was attached to the loading direction of the lamina. The specimen was also loaded step by step via the test machine and G_{12} was obtained by the measurement of the strain in the tensile direction ε_x [21]. G_{12} was calculated as:

$$G_{12} = \frac{1}{(4/E_x) - (1/E_1) - (1/E_2) + (2\nu_{12}/E_1)} \tag{3}$$

E_2, Y_t, and Y_c, are equal to E_1, X_t, and X_c, respectively, because of the woven structure. The mechanical properties of the woven-glass–polyester composite material are given in Table 2.

NUMERICAL ANALYSIS

Numerical analysis was performed by using the 3D finite element method with the assistance of a LUSAS 13.6 analysis program. Failure loads and failure modes of woven-glass–polyester composite laminated plates with two parallel circular holes were obtained by this program. Composite brick element (HX16L), which has 16 nodes, was selected during the numerical analysis. These element descriptions are generic element type (structural composite), element shape (hexahedral), and interpolation order (quadratic) [15]. The composite plate was modeled as a half model considering symmetry boundary conditions to reduce the solving time. The symmetry surface of the half model was supported on the XZ plane. Then, the hole surface of the plate was supported in the radial direction. Finally, tensile load was applied to the surface as shown in Figure 5. Hashin failure criteria was used to predict the failure map and the load increment strategy was defined for nonlinear solution.

RESULTS AND DISCUSSION

The failure behavior of two parallel pin loaded composite plates has been observed both experimentally and numerically for Groups 1 and 2. Three tests were realized for each type of specimen and average failure loads were calculated. All of the specimens were loaded to 6 mm displacement from the initial position during the experimental study.

According to tested specimens, three types of failure modes are observed as illustrated in Figure 6. First, the load usually reached a value between 1.0 mm and 1.5 mm displacement. Some specimens broke off suddenly at this point. This failure mode is known as net-tension (Figure 6(a)). For some specimens, the load decreases with increasing pin displacement. This failure mode is called shear-out (Figure 6(b)). Furthermore, the load increases with increasing of the pin displacement for a number of specimens. After the ultimate stage, the load decreases with growing failure. However, the specimen continues to carry loading. This failure mode is classified as bearing (Figure 6(c)). The load-carrying capacity of the joint during the bearing failure is higher than other failure modes, even if

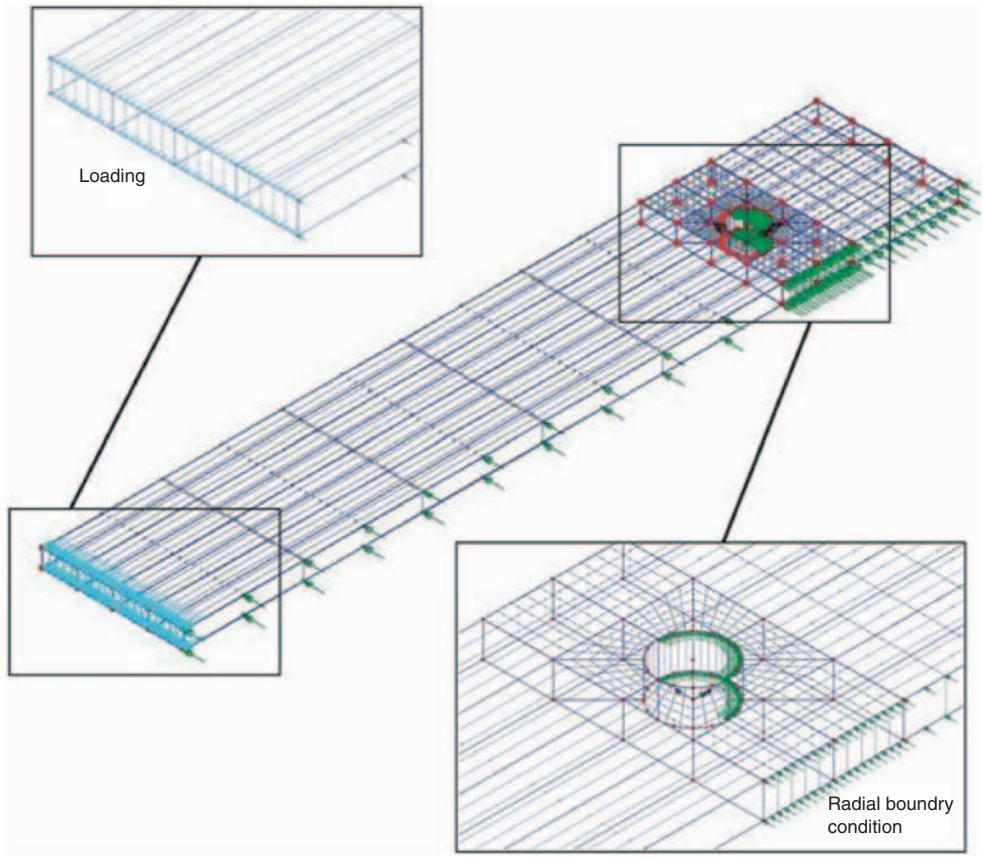

Figure 5. *Boundary conditions of the model when W/D = 8, E/D = 4 and M/D = 4.*

the pin joints carry on bearing load later than the first peak. From a safe design position, a bearing failure is more advantageous then either a shear-out or a net-tension failure [2,3]. Failure modes observed by the experimental and numerical studies are presented in Table 3 for all tested specimens. When $E/D = 1$ and 2, net-tension or shear-out failure modes occur for all M/D ratios, generally. The bearing failure modes are usually observed if $E/D = 3$, 4, and 5. In other words, the higher values of E/D ratio provide bearing failure mode. According to this table, the failure modes obtained for both experimental and numerical studies are seen to be very similar. Briefly, the failure modes are changing from shear-out to net-tension or bearing failure modes related to increasing E/D ratios. Increasing of E/D ratio produces the bearing failure modes.

The load-pin displacement curves of Groups 1 and 2 are shown in Figures 7 and 8, respectively. As seen from these figures, initially a linear slope occurs for all geometric parameters. Following this, the load generally decreases for $E/D = 1$ and increases for $E/D = 2$–5 ratios with increasing displacements for two group specimens. When $E/D = 1$, the curves reach the peak point and the points are equal to the ultimate bearing strengths. The slopes of the curves increase after the first peak and reach higher ultimate bearing strengths when the E/D ratio is equal to 2 or greater values. These figures point out that the magnitude of failure loads increase by increasing E/D ratio. Consequently, the higher values of failure loads are obtained for $E/D = 4$ or 5, generally. Moreover, the effects of

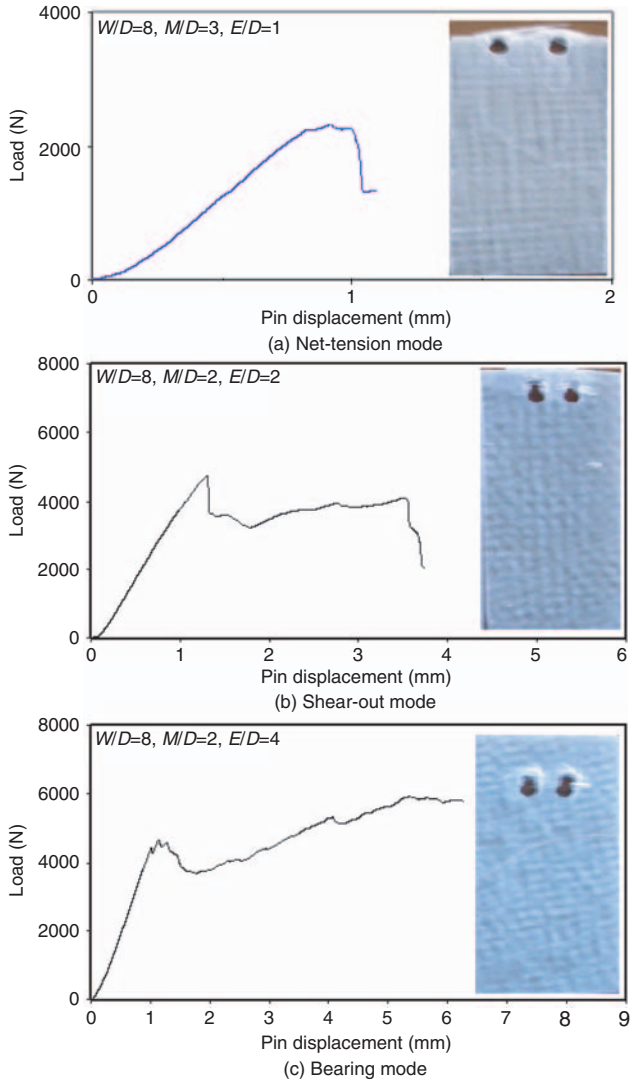

Figure 6. *Failure modes in experimental study.*

E/D ratio on bearing strengths are illustrated in Figure 9. The magnitudes of maximum failure loads for all tested specimens were obtained using load–displacement curves and then the bearing strengths of specimens were calculated by using Equation (1). This figure indicates that the values of bearing strengths rise with rising E/D ratio. However, this increase is very slow when $E/D = 3$ and higher values. The maximum value of bearing strengths is calculated as 456.94 MPa for Group 1 when $E/D = 4$ and $M/D = 3$, whereas the minimum value is computed as 95,52 MPa for Group 1 when $E/D = 1$ and $M/D = 4$. Nonetheless, the magnitudes of bearing strengths for Group 2 specimens are higher than Group 1 specimens, generally. It is understood that the magnitudes of failure loads and bearing strengths are strictly affected from geometrical parameters and orientations of laminated plates. When $E/D = 1$, the load carrying capacity of two parallel pinned composite joints is much lower than other E/D ratios, especially.

Table 3. Failure modes observed by the experimental and numerical studies.

		Group 1		Group 2	
***W/D* = 8**	***E/D***	**Experimental**	**Hashin**	**Experimental**	**Hashin**
M/D = 2	1	S	S	S	N
	2	N	N	N	N
	3	N	B	N	B
	4	B	B	B	B
	5	B	B	B	B
M/D = 3	1	S	S	S	N
	2	N	B	S	B
	3	N	B	B	B
	4	B	B	B	B
	5	B	B	B	B
M/D = 4	1	S	S	S	N
	2	S	S	S	S
	3	B	B	B	B
	4	B	B	B	B
	5	B	B	B	B
M/D = 5	1	S	S	S	N
	2	S	B	N	B
	3	B	B	B	N
	4	B	B	B	B
	5	B	B	B	B

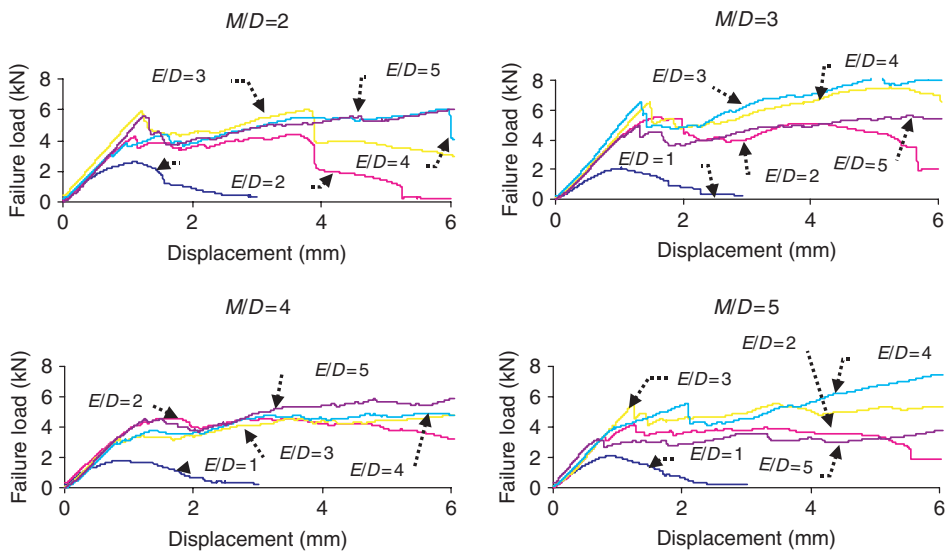

Figure 7. *Load-pin displacement curves of Group 1.*

The comparisons of maximum failure loads were obtained both of experimental and numerical studies for Groups 1 and 2 and are presented in Figure 10. It is clearly seen that experimental results are higher than numerical results for each analyzed specimen. However, experimental and numerical results are very close except for some specimens. The differences between experimental and numerical results can be neglected, generally.

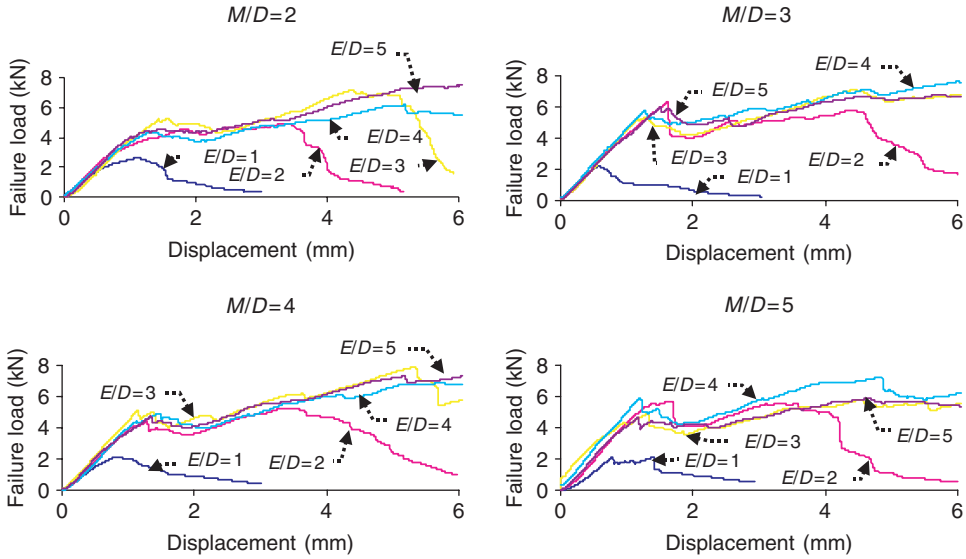

Figure 8. *Load-pin displacement curves of Group 2.*

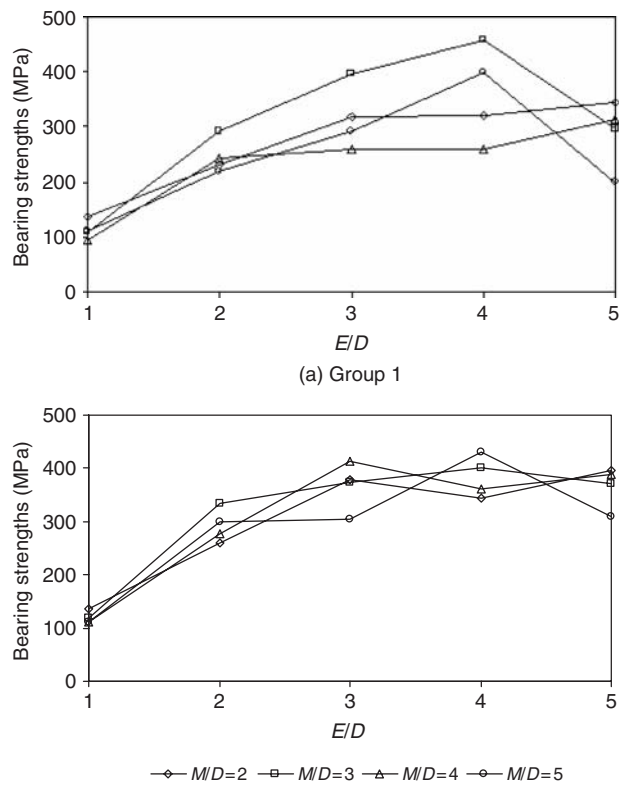

Figure 9. *The effect of E/D ratio on bearing strengths.*

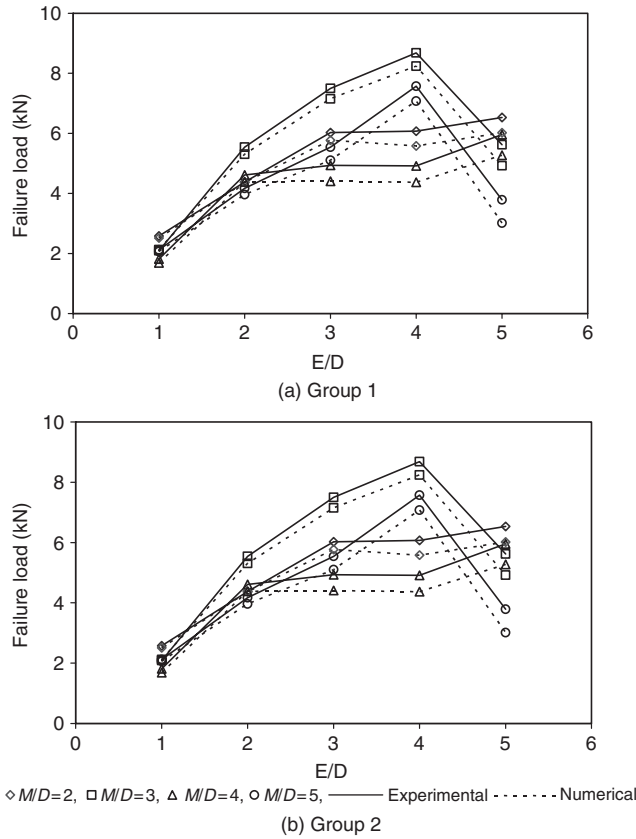

Figure 10. *Comparisons of numerical and experimental failure loads.*

CONCLUSIONS

According to experimental and numerical study results, the following remarks are summarized:

1. The values of bearing strengths of the composite plate are increased by increasing the geometric parameters such as E/D (free edge of the plate to hole diameter ratio) and M/D (the distance between two parallel holes to hole diameter ratio).
2. When $E/D = 1$ and 2, the bearing strength is small and failure mode is shear-out or net-tension observed in the weakest mode. When $E/D = 3$, 4, and 5, the bearing strengths are close to each other and the failure mode is generally known as the best failure mode of the resisting load.
3. During the net-tension and shear-out failure modes, the load reduces suddenly. However, in bearing failure modes, the load does not drop suddenly. Therefore, the pinned joints are stronger and safer if they are damaged as bearing.
4. The load-carrying capacity of $[0^\circ_2/60^\circ_2/]_s$ specimens are better than $[0^\circ]_8$ specimens, generally.
5. The obtained experimental and numerical failure modes are generally different, especially for $(E/D) = 1$, 2, and 3. In contrast, when $(E/D) = 4$ and 5, experimental and numerical failure modes are closer.
6. It is observed that the numerical and experimental analyses are in good agreement.

ACKNOWLEDGMENTS

This study was funded by Balikesir University under project number 2007/01. The authors express their thanks to Izoreel Firm in Izmir, Turkey. Special thanks to Dokuz Eylul University Mechanical Engineering Department, particularly Professor Onur Sayman, for their help and thoughts. Furthermore, we sincerely thank Filiz Özkan for her support.

REFERENCES

1. Tong, L., Mouritz, A. P. and Bannister, M. K. (2002). *3D Fibre Reinforced Polymer Composites*, **1st edn**, Elsevier.
2. Pakdil, M., Sen, F., Sayman, O. and Benli, S. (2007). The Effect of Preload on Failure Response of Glass-epoxy Laminated Composite Bolted-joints with Clearance, *Journal of Reinforced Plastics and Composites*, **26**: 1239–1252.
3. İcten, B. M. and Sayman, O. (2003). Failure Analysis of Pin-loaded Aluminum–Glass–Epoxy Sandwich Composite Plates, *Composites Science and Technology*, **63**: 727–737.
4. Aktas, A. (2005). Bearing Strength of Carbon Epoxy Laminates Under Static and Dynamic Loading, *Composite Structures*, **67**: 485–489.
5. Tercan, M., Asi, O. and Aktas, A. (2007). An Experimental Investigation of the Bearing Strength of Weft-knitted 1*1 Rib Glass Fiber Composites, *Composite Structures*, **78**: 392–396.
6. Yilmaz, T. and Sinmazcelik, T. (2007). Investigation of Load Bearing Performances of Pin Connected Carbon/polyphenylene Sulphide Composites Under Static Loading Conditions, *Materials and Design*, **28**: 520–527.
7. Caprino, G., Squillance, A., Giorleo, G., Nele, L. and Rossi, L. (2005). Pin and Bolt Bearing Strength of Fibreglass/aluminium Laminates, *Composites: Part A*, **36**: 1307–1315.
8. Kelly, G. and Hallström, S. (2004). Bearing Strength of Carbon Fibre/Epoxy Laminates: Effects of Bolt-hole Clearance, *Composites: Part B*, **35**: 331–343.
9. Xiao, Y. and Ishikawa, T. (2005). Bearing Strength and Failure Behavior of Bolted Composite Joints (Part I: Experimental Investigation), *Composites Science and Technology*, **65**: 1022–1031.
10. Xiao, Y. and Ishikawa, T. (2005). Bearing Strength and Failure Behavior of Bolted Composite Joints (Part II: Modeling and Simulation), *Composites Science and Technology*, **65**: 1032–1043.
11. Dano, M. L., Kamal, E. and Gendron, G. (2007). Analysis of Bolted Joints in Composite Laminates: Strains and Bearing Stiffness Predictions, *Composite Structures*, **79**: 562–570.
12. Camanho, P. P. and Lambert, M. A. (2006). Design Methodology for Mechanically Fastened Joints in Laminated Composite Materials, *Composites Science and Technology*, **66**: 3004–3020.
13. Whitworth, H. A., Aluko, O. and Tomlinson, N. A. (2008). Application of the Point Stress Criterion to the Failure of Composite Pinned Joints, *Engineering Fracture Mechanics*, **75**: 1829–1839.
14. Okutan, B. (2002). The Effects of Geometric Parameters on the Failure Strength for Pin-loaded Multi-directional Fiber-glass Reinforced Epoxy Laminate, *Composites: Part B*, **33**: 567–578.
15. Karakuzu, R., Çalışkan, C. R., Aktaş, M. and İçten, B. M. (2008). Failure Behavior of Laminated Composite Plates with Two Serial Pin-loaded Holes, *Composite Structures*, **82**: 225–234.
16. Chang, F. K., Scott, R. A. and Springer, G. S. (1982). Strength of Mechanically Fastened Composite Joints, *Journal of Composite Materials*, **16**: 470–494.
17. Sayman, O., Siyahkoc, R., Sen, F. and Ozcan, R. (2007). Experimental Determination of Bearing Strength in Fiber Reinforced Laminated Composite Bolted-joints Under Preload, *Journal of Reinforced Plastics and Composites*, **26**: 1051–1063.
18. ASTM D 3039-76, (1982). Test Method for Tensile Properties of Fiber-resin Composites, *American Society for Testing of Materials*.
19. Gibson, R. F. (1994). *Principals of Composite Material Mechanics*, McGraw-Hill, New York.
20. Tsai, H. H., Morton, M. Y. and Farley, G. L. (1991). An Experimental Investigation of Iosipescu Specimen for Composite Materials, *Journal of Experimental Mechanics*, 328–336.
21. Jones, R. M. (1999). *Mechanics of Composite Materials*, Taylor & Francis, Philadelphia.